A SHAPE MEMORY ALLOY OSCILLATOR: REGULAR AND CHAOTIC BEHAVIOR, USING BASIN OF ATTRACTIONS APPROACH

Vinícius Piccirillo, pcmec@ita.br
Luiz Carlos Sandoval Goes, goes@ita.br
Department of Enginnering Aeronautical and Mechanical, Tecnological Institute of Aeronautics – ITA, 12228 – 900, Sao Jose dos Campos, SP, Brazil

José Manoel Balthazar, jmbaltha@rc.unesp.br
Department of Statistic, Applied Mathematical and Computation, Sao Paulo State University – UNESP, 13500 – 230, Rio Claro, SP, Brazil

Abstract. *Shape Memory Alloy (SMA) consists itself of a group of metallic materials, which demonstrates the ability to return to some previously defined shape, when it is subjected to the appropriate thermal procedure. In this paper the classical nonlinear behaviors and global bifurcation of a SMA oscillator system subject to harmonic excitation, were investigated. The global bifurcation analyses with the variation of excitation amplitude and temperature were carried out respectively and some bifurcation diagrams were presented. The authors numerically investigate basins of attraction of periodic attractors in this model. These attractors are strongly dependent on small changes of the initial conditions. Gradually varying a control parameter, the size of these basins of attraction is modified by global bifurcations of their boundaries.*

Keywords*: Chaos, Shape Memory Alloy, Nonlinear Dynamics, Basin of Attraction*

1. INTRODUCTION

Shape memory alloy (SMAs) refer to a group of materials, which have the ability to return to a predetermined shape when they are heated. The source of the distinctive mechanical behavior of these materials is a crystalline phase transformation between a high symmetry, highly ordered parent phase (austenite), and a low symmetry, less ordered product phase (martensite).

The phenomena related to the shape memory alloys (SMA) are associate to the transformations of the phase, which can be caused by the variation of the temperature, as well as, for the variation in the tension level. Basically, the SMA presents two stable phases: austenite and martensite.

According to the mechanical behavior, the shape memory alloys, may be divided in two categories: shape memory (SME) and pseudoelastic effect. Shape memory effect is related to the ability of the material to recover a great quantity of the residual strain, caused for the action of a loading and unloading, through of the increasing of the temperature of the material, in this situation the martensitic phase s stable. Already, the pseudoelasticity behavior refers to the ability of the material to obtain a very large strain upon loading and fully recover through a hysteresis loop upon loading and always occurs in high temperatures, in this situation the austenitic phase is stable.

The dynamical response of the shape memory systems is introduced in different references (Lacarbonara et. al. 2004), (Savi et. al. 2008), (Piccirillo et. al. 2009), without deserve others. Recently, some experimental analyses confirm the presence of chaos in shape memory systems, Mosley and Mavroidis (2001). Chaotic behavior is an interesting nonlinear phenomenon, which has been intensively studied during the last three decades. Chaotic behavior is commonly detected in a wide variety of physical systems, such as electrical, mechanical, and thermal systems, Nayfeh (1994). A fundamental characteristic of chaotic systems is its unpredictability.

Computing basins of attraction results in a new understanding of the behavior of dynamical system. The basin of attraction of an attracting set is the set of all the initial conditions, in the phase space whose trajectories go to that attracting set. Nusse et. al. (1997).

Souza et. al. (2008) considers a gear box model and discussed the coexistence of attractors with fractal basin boundaries, as well as the existence of long chaotic transients. Souza et. al. (2005) study the effect of the amplitude constraint it is to modify the basin boundary structure in a nondeial problem.

The aim of this paper is to analyze the bifurcation of the SMA oscillator. For this system, we initially determine the coexisting periodically attractors and then analyze their basins of attraction.

2. SMA CONSTITUTIVE MODEL

To describe the behavior of the oscillator with shape memory, we adopt in the mathematical modeling of the problem the constitutive model proposed, as an example by Savi and Braga (1993).This model is based on Devonshire theory and it defines a free energy of Helmholtz (ψ) in the polynomial form and it is capable to describe the shape memory and pseudoelasticity effects. The polynomial model is more known to deal with one–dimensional cases and it

does not consider an explicit potential of dissipation, and no internal variable is considered. In this form, the free energy depends only on the state variable (temperature and strain), that is, $\psi = \psi(\varepsilon, T)$

The free energy is defined in such a way that, for high temperatures ($T > T_A$), the energy possesses only one point of minimum corresponding to the null strain representing the stability of the austenite phase (A); for intermediate temperatures ($T_M < T < T_A$), it presents three points of minimum corresponding to the phases austenitic (A), and two other martensitic phases (M^+ and M^-), which are induced by positive and negative stress fields, respectively; for low temperatures ($T < T_M$), there are two points of minimum representing the two variants of martensite (M^+ e M^-), corresponding to the null strain.

Therefore, the above restrictions are given by the following equation polynomial:

$$\rho\psi(\varepsilon,T) = \frac{1}{2}q(T - T_M)\varepsilon^2 - \frac{1}{4}b\varepsilon^4 + \frac{1}{6}e\varepsilon^6 \tag{1}$$

where *q* and *b* are constants of the material, T_A corresponds to the temperature where the austenite phase is stable, T_M corresponds to the temperature where the martensitic phase is stable and ρ is the mass density; and the free energy has only one minimum at zero strain:

$$T_A = T_M + \frac{b^2}{4qe} \tag{2}$$

and the constant *e* may be expressed in terms of other constants of the material. Thus, the stress–strains relation is given by

$$\sigma = q(T - T_M)\varepsilon - b\varepsilon^3 + \frac{b^2}{4q(T_A - T_M)}\varepsilon^5 . \tag{3}$$

According to Paiva and Savi (2006) the polynomial model represents both martensite detwinning process and pseudoelasticity in a qualitatively coherent way, although it does not consider a twinned martensite (M). In other words, there is no stable phase for $T < T_M$ in a stress-free state, but the authors believe that this analysis is useful for the understanding of the nonlinear dynamics of shape memory systems. The proposed model captures all of the essential features of the studied phenomenon.

3. THE PROBLEM

We consider the one-degree-of-freedom-oscillator, which consists of a mass *m*, connected to a rigid support through of a viscous damping with coefficient *c* and a shape memory element, where a periodic external force $p(t) = p\cos(\omega t)$, is applied to the systems, as shown in figure 1.

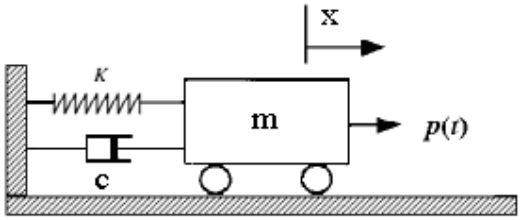

Figure 1: Model of a SMA oscillator with ideal excitation

Thus, the equation of motion that governs the vibrating system, may be written as,

$$m\frac{d^2x}{dt^2} + c\frac{dx}{dt} + K(x,T) = p\cos(\omega t) \tag{4}$$

On the other hand, the behavior of the element, with shape memory, can be described through the constitutive model polynomial. Therefore, the restoring force of the spring is given by,

$$K = K(x,T) = \bar{q}(T - T_M)x - \bar{b}x^3 + \bar{e}x^5 \tag{5}$$

where,

$$\bar{q} = \frac{qA_r}{L}; \qquad \bar{b} = \frac{bA_r}{L^3}; \qquad \bar{e} = \frac{eA_r}{L^5} \tag{6}$$

It follows that x represents the variable relative to the displacement of the element with shape memory; L is the length and A_r is the area of this element.

Then, the governing equation of motion of the oscillator is given by

$$m\frac{d^2x}{dt^2} + c\frac{dx}{dt} + \bar{q}(T - T_M)x - \bar{b}x^3 + \bar{e}x^5 = p\cos(\omega t) \tag{7}$$

Next, we introducing the following dimensionless variables

$$y = \frac{x}{L} \qquad and \qquad \tau = \omega_0 t \tag{8}$$

Eq. (7) becomes

$$\ddot{y} + 2\mu\,\dot{y} + (\theta - 1)y - \alpha\,y^3 + \gamma\,y^5 = \delta\cos(\phi\tau) \tag{9}$$

where the dot represents time differentiation and the dimensionless variables are given by,

$$\mu = \frac{c}{2m\omega_0}, \quad \theta = \frac{T}{T_M}, \quad \alpha = \frac{bA}{mL\omega_0^2}, \quad \gamma = \frac{eA}{mL\omega_0^2}, \quad \delta = \frac{p}{mL\omega_0^2}, \quad \phi = \frac{\omega}{\omega_0}, \quad \omega_0^2 = \frac{qAT_M}{mL} \tag{10}$$

Eq. (9) can be rewritten as three coupled first-order differential equations

$$\begin{aligned} \dot{y}_1 &= y_2 \\ \dot{y}_2 &= \delta\cos(y_3) - 2\mu\,y_2 - (\theta - 1)y_1 + \alpha\,y_1^3 - \gamma\,y_1^5 \\ \dot{y}_3 &= \phi \end{aligned} \tag{11}$$

4. NUMERICAL SIMULATIONS

The numerical simulation results, presented here were obtained using the fourth-order Runge–Kutta algorithm, with variable stelenght. In all simulations, we have used the material properties presented in Table 1. Assuming also that the SMA element has the following values: $A_r = 1.96\times10^{-5}\,m^2$, $L = 50\times10^{-3}\,m$, and unitary mass.

Table 1: Material constants for a Cu-Zn-Al-Ni alloy [27]

q (MPa/K)	b (MPa)	e (MPa)	T_M (K)	T_A (K)
523.29	1.868×10^7	2.188×10^9	288	364.3

In addition to the sensitive dependence on the initial conditions, a dynamical system is very sensitive to small variations in the control parameters. As a control parameter varies, the stability of a dynamical system changes, due to a local or a global bifurcation. The bifurcation diagram provides a general view of the system dynamics, by plotting a system variable, as a function of a control parameter, Alligood et. al. (1996). Fig. 2 show a global view of the bifurcation diagram of the SMA nonlinear model described by Eq. (9), where we have kept four control parameter μ, γ, α and $\theta = 0.7$ (where the martensitic phase is stable) fixed, and only vary the forcing amplitude δ. For a given

control parameter δ, the bifurcation diagram Fig. 2 plots the asymptotic values of the Poincaré points of the system variable y, where the transient has been omitted.

To build this figure, we start with $\delta = 0.1$ and a random initial condition for the state variable $y = (y_{01}, y_{02}, y_{03})$. We then plot the values of y_{01} for 200 Poincaré points of the trajectory of y, after discarding 200 points of the initial transient. Next, we increase δ by a small amount and, using the current value of y, as the new initial condition, we then drop the first 200 Poincaré points and plot the following 200 Poincaré points of a new trajectory. We repeat this procedure until $\delta = 0.4$. In this way, we follow the dynamics of the SMA system as δ is varied. If we use different random initial conditions for a given value of δ, we may find other attractors in the phase space (y_1, y_2), since those initial conditions might fall in different basins of attraction. The rich dynamical states displayed by the bifurcation diagram indicate that a dynamical system is sensitively dependent on a small variation of its control parameters.

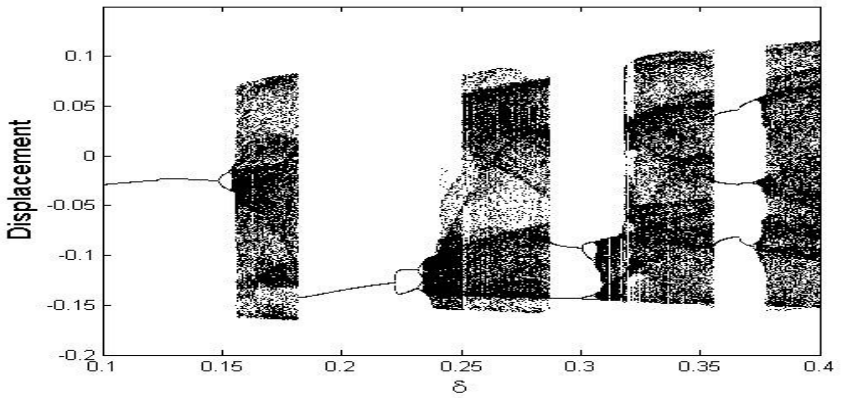

Figure 2: Bifurcation Diagram for $\theta = 0.7$

Evidently, multistability is a fundamental feature of a complex system, as seen in the periodic window of the bifurcation diagram in Fig. 2. The basin of attraction for a given attractor it is the set of initial conditions, each of which gives rise to a trajectory that converges asymptotically to the attractor, Hilborn (1994).

Multistability is a basic feature of complex dynamical systems whereby two or more attractors can coexist for a given value of the control parameter. This is depicted by the basins of attraction in Fig. 2, for an example, in interval $0.221 \le \delta \le 0.232$, two attractors coexist each attracts a different set of initial conditions in the phase space. In Fig. 3, we plot the basins of attraction for first attractor in white color and second attractor in black color at $\delta = 0.2242$. To find the basins of attraction, we define a grid of 641×641 points in the phase space and iterate each point of the grid until it reaches one of the attractors. We color the initial condition according to the attractor to which its trajectory converges. It can be seen that most initial conditions are attracted to black color.

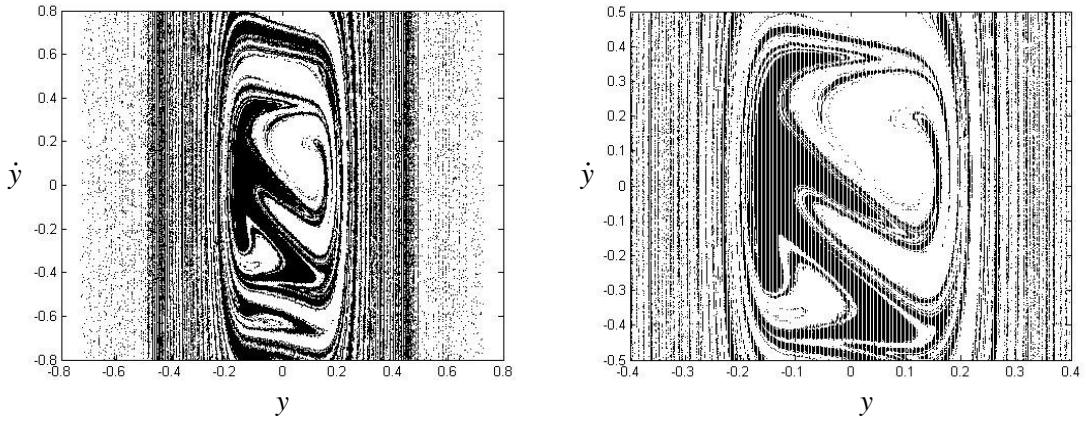

(a) (b)

Figure 3: Basin of attraction, (a) for the two periodic attractor in white color and black color and (b) Zoom of the figure (a)

In Fig. 4, the bifurcation diagram for the amplitude ratio as a control parameter it is investigated considering $\theta = 2$. When $\delta \approx 0.26$ the system loses stability and there is a period-doubling bifurcation and unsymmetrical motion occurs. Thereafter, the motion undergoes a succession of period-doubling bifurcations with decrease in δ, which eventually result in apparently non-periodic or chaotic motions.

Some regions of these basins have highly interleaved fractal boundaries. To show this characteristic, we present in Figure 3(b) a zoom of Figure 3(a). Figure 3(b) shows the coexistence of the two attractors and fine structures at any phase space scale. Consequently, there are regions for which the system's behavior is strongly dependent on small changes of initial conditions.

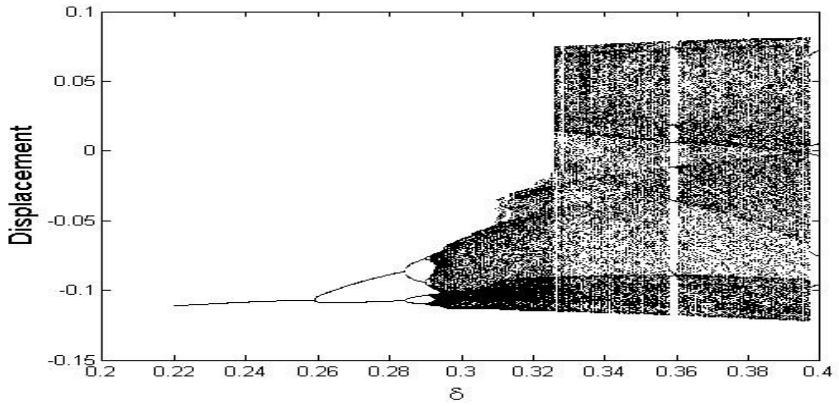

Figure 4: Bifurcation Diagram for $\theta = 2$

In Fig. 4, for an example, in interval $0.259 \le \delta \le 0.2842$, two attractors coexist each attracts a different set of initial conditions, in the phase space. In Fig. 5, we plot the basins of attraction for first attractor in white color and second attractor in black color at $\delta = 0.2701$. To find the basins of attraction, we define a grid of 641×641 points in the phase space and iterate each point of the grid until it reaches one of the attractors. We color the initial condition according to the attractor to which its trajectory converges. It can be seen that most initial conditions are attracted to black color.

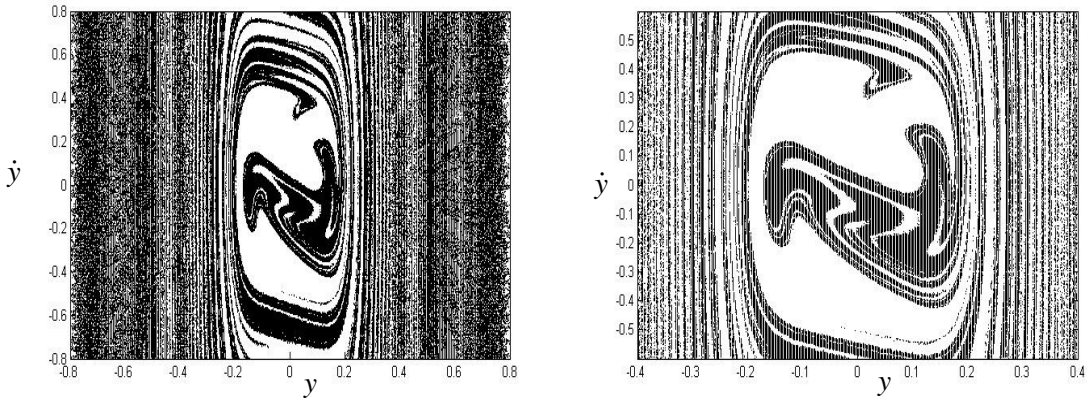

(a) (b)

Figure 5: Basin of attraction: (a) for the two periodic attractor in white color and black color and (b) Zoom of the figure (a), where $\delta = 0.2701$

In Fig. 4, for an example, in interval $0.2842 \le \delta \le 0.2896$, four attractors coexist each attracts a different set of initial conditions in the phase space. In Fig. 6, we plot the basins of attraction for first attractor in white color, second attractor in black color, third attractor in blue color and fourth attractor in red color at $\delta = 0.2701$. To find the basins of attraction, we define a grid of 641×641 points in the phase space and iterate each point of the grid until it reaches one of the attractors. We color the initial condition according to the attractor to which its trajectory converges. It can be seen that most initial conditions are attracted to red color.

Fig. 7 provides an illustration how the temperature θ influences the system dynamics.

For values of temperature in the wide range of parameter, the SMA oscillator demonstrates a chaotic behavior, which then after a cascade of subcritical period doubling bifurcations ends up with a period two motion and soon after a one period.

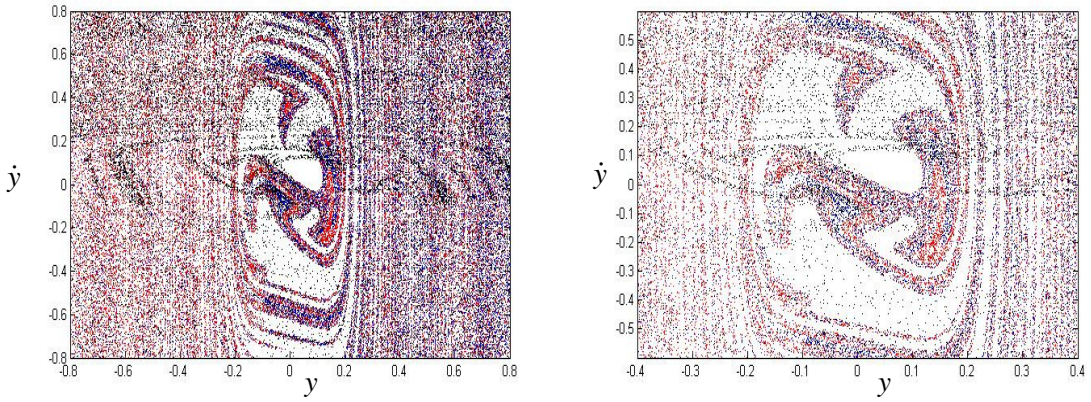

(a) (b)

Figure 6: Basin of attraction: (a) for the four periodic attractor in white, black, blue and red colors and (b) Zoom of the figure (a), where $\delta = 0.286$

In Fig. 7, for an example, in interval $0.8172 \le \delta \le 0.8982$, two attractors coexist each attracts a different set of initial conditions in the phase space. In Fig. 8, we plot the basins of attraction for first attractor in white color and second attractor in black color at $\delta = 0.8451$. To find the basins of attraction, we define a grid of 641×641 points in the phase space and iterate each point of the grid until it reaches one of the attractors. We color the initial condition according to the attractor to which its trajectory converges. It can be seen that most initial conditions are attracted to black color.

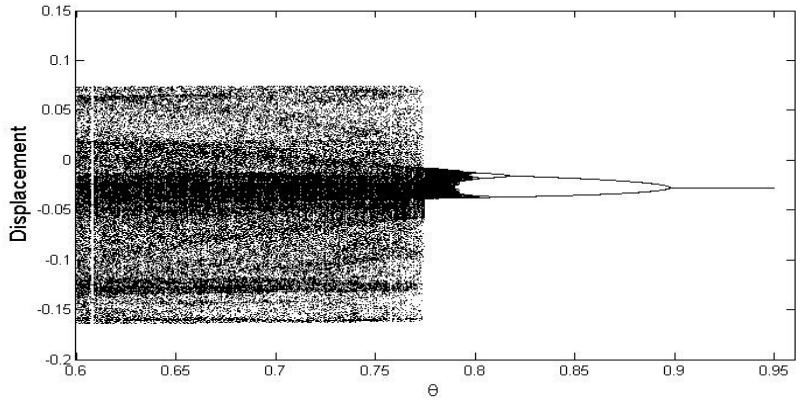

Figure 7: Bifurcation Diagram for $\delta = 0.1$

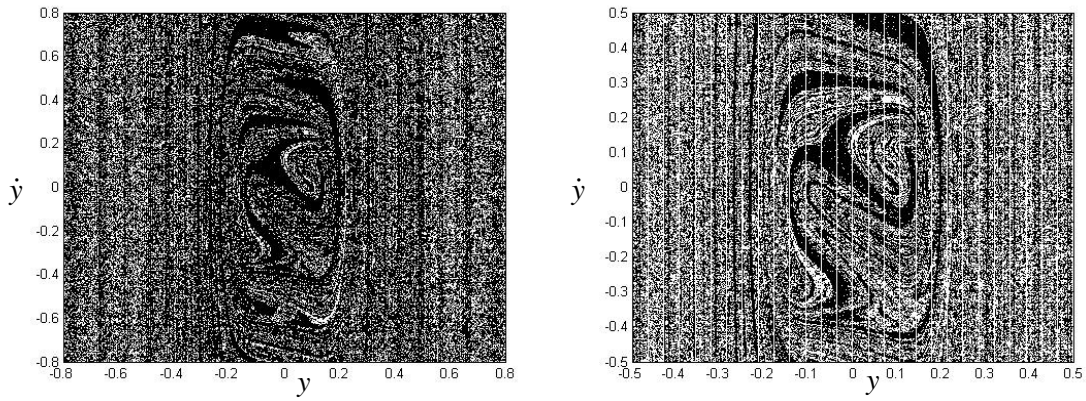

(a) (b)

Figure 8: Basin of attraction, (a) for the four periodic attractor in white, black, blue and red colors and (b) Zoom of the figure (a), where $\delta = 0.286$

5. CONCLUSION

In this paper a numerical study of nonlinear dynamics of a SMA oscillator it is presented. The analysis it is developed by considering different temperature sets for the shape memory element.

Depending on the parameter configuration, the system displays various dynamical responses. The bifurcation diagrams and basins of attraction were used to examine the system dynamics.

In terms of the system dynamics our analysis shows that, as the control parameters are varied, a complex SMA system undergoes a variety of dynamic transitions which change its stability properties, namely, local bifurcations such as period-doubling bifurcation. Moreover, the topology of the basins of attraction is modified by global bifurcations of their boundaries.

In any case it is of practical importance to investigate the basins of attraction related in the different situations, since we can determine to what extent a small uncertainty in the initial condition reflects on the knowledge of the attractor the system will asymptote to.

The basins of each behaviour are densely mixed and, as suggested by the magnification shown in Figs. 3b, 5b, 6b and 8b, the basin boundary looks like a fractal curve.

Furthermore, for the considered control parameter range, the basin boundaries are fractals and so interleaved that the trajectory might deviate from one basin to another.

6. ACKNOWLEDGEMENTS

The authors thank the support of the Brazilian government agency CNPq.

7. REFERENCES

Alligood, K.T., Sauer, T.D., Yorke, J.A., 1996, "Chaos: an introduction to dynamical systems". New York: Springer-Verlag.

Hilborn, R.C., 1994, "Chaos and nonlinear dynamics: an introduction for scientists and engineers". New York: Oxford University Press

Lacarbonara, W., Bernardini, D., Vestroni, F., 2004, "Nonlinear Thermomechanical Oscillations of Shape Memory Devices". International Journal of Solids and Structures, Vol. 41, PP. 1209–1234.

Mosley, M.J., Mavroidis, C., 2001, "Experimental nonlinear dynamics of a shape memory alloy wire bundle actuator". J. Dyn. Syst. Meas. Control Vol. 123, pp. 103–123.

Nayfeh, A.H., 1994, "Applied Nonlinear Dynamics". Wiley, New York.

Nusse, H.E., Yorke, J.A., Hunt, B.R., Kostelich, E.J., 1997, "Dynamics: Numerical Explorations", Springer – Verlag.

Paiva, A., Savi, M.A., 2006, "An Overview of Constitutive Models for Shape Memory Alloy", Mathematical Problem in Engineering, Vol. 2006, pp. 1 – 30.

Piccirillo, V., Balthazar, J.M., Pontes Jr., B.R., Felix, J.L.P., 2009, "Chaos Control of a Nonlinear Oscillator with Shape Memory Alloy Using an Optimal Linear Control: Part I: Ideal Energy Source", Nonlinear Dynamics, Vol. 55, pp. 139 – 149.

Savi, M., and Braga, A.M.B., 1993, "Chaotic Vibrations of an Oscillator with Shape Memory", Journal of the Brazilian Society of Mechanical Sciences and Engineering, Vol. XV, pp. 1 – 20.

Savi, M., Sá, M.A.N., Paiva, A., Pacheco, P.M.C.L., 2008, "Tensile-Compressive Asymmetry Influence on Shape Memory Alloy System Dynamics". Chaos, Solitons and Fractals, Vol. 36, pp. 828–842.

Souza, S.T.L., Caldas, I.L., Viana, R.L., Balthazar, J.M., Brasil, R.M.L.R.F., 2005, "Basins of Attraction Changes by Amplitude Constraining of Oscillator with Limited Power Supply", Chaos, Solitons and Fractal, Vol. 26, pp. 1211 – 1220.

Souza, S.T.L., Caldas, I.L., Viana, R.L., Balthazar, J.M., 2008, "Control and Chaos for Vibro-Impact and Nonideal Oscillator", Journal of Theoretical and Applied Mechanics, Vol. 46, pp. 641 – 664.

8. RESPONSIBILITY NOTICE

The authors are the only responsible for the printed material included in this paper.